

Food & Function

Accepted Manuscript



This is an *Accepted Manuscript*, which has been through the Royal Society of Chemistry peer review process and has been accepted for publication.

Accepted Manuscripts are published online shortly after acceptance, before technical editing, formatting and proof reading. Using this free service, authors can make their results available to the community, in citable form, before we publish the edited article. We will replace this *Accepted Manuscript* with the edited and formatted *Advance Article* as soon as it is available.

You can find more information about *Accepted Manuscripts* in the [Information for Authors](#).

Please note that technical editing may introduce minor changes to the text and/or graphics, which may alter content. The journal's standard [Terms & Conditions](#) and the [Ethical guidelines](#) still apply. In no event shall the Royal Society of Chemistry be held responsible for any errors or omissions in this *Accepted Manuscript* or any consequences arising from the use of any information it contains.

23 Introduction

24 Enriching staple foods and beverages with nutraceuticals is a promising approach for promoting
25 health of broad populations. However, the enrichment with hydrophobic nutraceuticals is highly
26 challenging due to their low water solubility, poor bioavailability and high sensitivity to degradation
27 during production, shelf life and digestion.¹ Nanoparticle-based delivery systems, which can
28 circumventing the pitfalls of poor water solubility and chemical instability, are very suitable for
29 hydrophobic nutraceuticals.² Plant proteins (mainly soy proteins, zein and wheat gliadins) are widely
30 available, low-cost and safer (less allergenic and low possibility to provoke zoonotic disease
31 transmission). More importantly, they can be easily made into food colloidal delivery systems based
32 on the occurrence of non-covalent interactions (including hydrophobic interactions, hydrogen
33 bonding, electrostatic interactions, and aromatic stacking) with bio-active substances.³

34 Zein, a hydrophobic prolamine, contains a large number of hydrophobic amino acids. The inherent
35 amphiphilic property of zein makes it a fine material in fabricating functional colloidal particles and
36 controlling the release of drugs and nutritional supplements.^{4,5} By simple anti-solvent precipitation
37 method,⁶ many alcohol-soluble bioactive ingredients, such as polyphenols (thymol⁷, curcumin⁸,
38 quercetin⁹ and cranberry procyanidins¹⁰) and essential oils¹¹ have been encapsulated into zein
39 particles because of their co-dissolution in water-alcohol solutions. This could hugely improve the
40 chemical stability of such bioactive ingredients and the bioavailability through controlled-release *in*
41 *vivo*. However, since zein colloidal particles are stabilized by surface repulsion (electrostatic
42 stabilization), they tend to lose physical stability when approaching neutral pH and physiological pH
43 in intestine, both leading to particles aggregation.¹² To overcome the drawbacks, stabilizers like
44 sodium caseinate⁶ or gum arabic¹³ have been added to water solution. Unfortunately, zein colloidal

45 particles are usually in large scale (diameter >100 nm), and they are commonly turbid dispersions in
46 aqueous phase, which greatly limit their applications in some food processing fields (e.g., clear
47 drinks).

48 The self-assembly of amphiphilic polypeptides have attracted many attentions in recent years.
49 Various nanostructures, such as micelles, nanotubes, nanofibers and nanoribbon, could be fabricated
50 by the self-assembly of amphiphilic peptides.¹⁴ Such nanostructures, as delivery vehicles, have great
51 potential applications in transport and delivery of bioactive compounds, nutrients or additives.³
52 Synthetic amphipathic proline-rich peptides based on N-terminal domain of γ -zein exhibited a
53 prominent characteristic as a new carrier in nanotechnology.¹⁵ Moreover, some amphiphilic protein
54 hydrolysates, such as α -lactalbumin hydrolysate¹⁶, were also found to have the self-assembling
55 properties.

56 Proline-rich zein contains numerous amphipathic polypeptide fragments. However, there has
57 been no report on the amphipathic characteristic of ZH and its applications as a nanocarrier. Studying
58 these issues could pave the way for many important applications, such as the entrapment and
59 protection of bioactive substance in food processing. In fact, we have recently found out that ZH
60 exhibited excellent amphiphilic and self-assembly properties in water solution, showing an enormous
61 potential in the application of food colloidal delivery systems. Curcumin (Cur), a hydrophobic
62 polyphenol derived from the rhizome of herb, is endowed with a number of biological and
63 pharmacological activities, such as antioxidant, anti-inflammatory, antimicrobial, and
64 anticarcinogenic.² However, due to poor water solubility and chemical instability, bioavailability of
65 Cur is hugely limited, impeding its conversion from cooking to clinical and functional foods
66 applications.¹⁷⁻¹⁹ The aim of this work was to study the amphiphilic properties of ZH, and a model

67 co-assembled nanocomplexes system based on ZH was established for the protected delivery of
68 curcumin. In particularly, the interactions between ZH and Cur were also studied using fluorescence
69 titration and FTIR methods.

70 **Materials and Methods**

71 **Materials**

72 Zein (>92%), Curcumin (~98% purity, from *Curcuma longa*) and pyrene (>99% purity) were
73 purchased from Sigma-Aldrich (St. Louis, MO). *Alcalase* 2.4L (endoproteinase from *Bacillus*
74 *licheniformis*, 2.4AU/g) was obtained from Novozymes North America Inc. (Franklinton, NC).
75 Sodium caseinate (Na-Cas) (>90%) was obtained from Meryer chemical technology Co., Ltd
76 (Shanghai, China). All other chemicals used were of analytical grade.

77 **Preparation and characterization of ZH**

78 ZH was prepared according to the method of *Kong, et al.*²⁰ with some modifications. Briefly, zein
79 suspension in deionized water (3% w/v) was hydrolyzed with *Alcalase* at 50 °C in automatic
80 potentiometric titrator (Metrohm). The enzyme to zein substrate ratio was 2:100 (mL/g). The pH of
81 zein suspension was adjusted to 9.0 before hydrolysis was initiated, and maintained at 9.0 by
82 continuously dropwise adding 1 M NaOH during hydrolysis. The process of enzymolysis was
83 terminated when pH didn't drop in 5 min. After hydrolysis, the pH was brought to 7.0 using 1 M HCl,
84 and the solution was then heated at 95 °C for 5 min to inactivate the enzyme. Then the hydrolysate
85 was centrifuged at 10, 000 r/min, 25 °C for 20 min. The supernatant was dialyzed (100 Da cutoff)
86 over night against deionized water and finally freeze-dried (Dura-Dry MP freeze-dryer, FTS Systems,
87 Inc., Ridge, NY). The prepared ZH was placed in the ziplock bags and stored at 4 °C before use. To
88 eliminate possible color interferences with the following chemical analyses, ZH solutions were

89 decolored by mixing with an equal volume of chloroform. The organic phase containing the
90 extracted pigments was removed.

91 Protein solubility in specified hydrolysis time points was measured according to the biuret
92 method²¹. ZH solutions were centrifuged at 1800 g for 10 min. Protein solubility (percent) was
93 defined as the protein amount in the supernatant divided by the original protein amount and then
94 multiplied by 100.

95 The degree of hydrolysis (DH) was monitored by the pH-Stat method.²² The amount of alkali
96 consumed in enzymatic reaction was recorded and used to calculate the DH. DH was calculated from
97 the following equation:

$$98 \quad \text{DH (\%)} = B \times N_b \times \alpha^{-1} \times (M)^{-1} \times (h_{\text{tot}})^{-1} \times 100$$

99 where B = base consumption (mL); N_b = base concentration (2N);

100 α^{-1} = average degree of dissociation of α -amino groups = 1.01; M = mass of protein (g); h_{tot} = total
101 number of peptide bonds in the protein substrate = 9.2 milli-equivalents/gram protein.

102 Native zein and its hydrolysates derived from specified time points were subjected to sodium
103 dodecyl sulfate-polyacrylamide gel electrophoresis (SDS-PAGE) as described by Laemmli.²³
104 Aliquots of 5 μ L samples were loaded in each well on the gel. A molecular weight (MW) standard
105 composed of a cocktail of proteins (14.4-97.40 kDa) (Bio-Rad Laboratories) was also run.

106 **Self-assembly properties and interfacial activity of ZH**

107 Critical micelle concentration (CMC) was determined based on intensity ratio of the first peak to
108 the third (I1/I3) of pyrene fluorescence spectrum during its entrapment in hydrophobic domains
109 forming upon micellization.²⁴ A series of decimal dilutions of ZH (0.01 up to 20 mg/mL) were
110 prepared using phosphate buffer solution (PBs, pH 7.2, 10 mM). The final concentration of pyrene in

111 each sample was 1.0 μM . Each spectrum was measured in the wavelength range 350-500 nm with
112 the excitation wavelength being 335 nm. The excitation and emission slit widths were set at 5 and
113 2.5 nm, respectively. The intensity ratio of I1 to I3 of the pyrene fluorescence spectrum showed the
114 micropolarity where the probe exists. The intensity ratios of I1 to I3 were plotted as a function of
115 logarithm of ZH concentrations. The data were fitted using the nonlinear fitting with Boltzman's
116 Curve. The CMC was obtained from the inflection point of the nonlinear fitting. As contrasts, ZHs
117 obtained after 1 h (ZH1) and 3 h (ZH3) enzymolysis were all carried out.

118 Dynamic interfacial adsorption of ZH at oil-water interface was determined by monitoring the
119 evolution of surface tension. An optical contact angle meter, OCA-20 (Dataphysics Instruments
120 GmbH, Germany) was used in a dynamic mode for measuring surface tension at the oil-water
121 interface at 25 °C. Details of this apparatus were given elsewhere.²⁵ The samples were diluted to 1
122 mg/mL with PBs (10 mM, pH 7.2), and placed in the syringe to reach the desired constant
123 temperature. Then a drop was delivered into a purified corn oil and allowed to stand for 2 h to
124 achieve protein adsorption. As contrasts, ZH1, ZH3, and Na-Cas at the same concentration (1 mg/mL)
125 were all carried out.

126 **Fabrication and characterization of ZH-Cur nanocomplexes**

127 Unless otherwise specified, ZH obtained after 3 h hydrolysis time was selected in the following
128 sections, to simplify the experimental process. 0.1 mL stock solution of Cur (3 mg/mL in ethanol)
129 was respectively added into 2.9 mL of ZH solutions (1, 2.5 and 5 mg/mL). The mixtures were
130 centrifuged at 10000 $\times g$, 4 °C for 20 min to pellet the unbound Cur, and the supernatants containing
131 Cur nanocomplexes were preserved in a light-resistant container at 4 °C for determination. As the
132 contrasts, ZH without Cur and Cur without ZH in the same PBs solution with homologous

133 concentration were also prepared.

134 UV-vis spectra were measured by UV-spectrophotometer (UV2300, ECHCOMP). Cur ethanol
135 solution (20 μ L, 3 mg/mL) was added into ZH solution (2.98 mL, 2.5 mg/mL) at room temperature.
136 Appropriate contrasts of ZH without Cur and of Cur without ZH were also tested.

137 To quantify the bound Cur in ZH solutions, the methodology according to Ma *et al.*²⁶ was adopted
138 with some modifications. Briefly, 100 μ L of freshly prepared nanocomplexes dispersion was added
139 to 900 μ L methanol in a tube. After a violent shaking, each sample was centrifuged at 15,000 \times g, 4°C
140 for 30 min, and the extracted supernatant was used for Cur quantification. Each sample was filtered
141 through a 0.22 μ m filter (Millipore, Billerica, MA, USA) prior to HPLC determination, then aliquots
142 of 20 μ L sample was injected to mobile phase (methanol) using a reversed column (C₁₈ column,
143 250 \times 4.5 mm, 5 μ m, Waters), and a UV detector at 425 nm. The flow rate was 0.5 mL/min. The
144 solubility of Cur in various zein hydrolysate solutions was quantified by the Cur standard curve ($Y =$
145 $0.44 X + 0.0015$, $R^2 = 0.9994$). Encapsulation efficiency (EE) was calculated as the percentage of
146 Cur in the supernatant with respect to the total added Cur. Analysis report was based on the results
147 obtained from three replicates of each sample.

148 The chemical stability of Cur was evaluated based on the methodology of Ma *et al.*²⁶. The freshly
149 prepared nanocomplexes dispersions containing sodium azide (0.002%, w/v) were incubated under
150 ambient conditions. As a contrast, free Cur was also dispersed in PBs by the same method. At
151 specified time points, samples (100 μ L) were taken out and added to 900 μ L of methanol for
152 quantitative analysis of Cur by RP-HPLC, as described above. The results were represented by
153 retained ratio of Cur, which was calculated as the percentage of retained Cur at certain time point
154 with respect to the initial value.

155 The particle size and surface charge of the nanocomplexes and ZH alone (2.5 mg/mL) were
156 measured using a commercial dynamic light scattering and micro-electrophoresis device (Malvern
157 Instruments Co. Ltd., Worcestershire, UK). The size distributions were calculated from the scattered
158 light intensity fluctuations by cumulant analysis of the autocorrelation function. Zeta potential was
159 reported on the basis of three replicates. All measurements were carried out at 25 °C.

160 The morphology of the nanocomplexes prepared in ZH solution (2.5 mg/mL) was observed using
161 XFlash 5030T transmission electron microscopy (Bruker, Germany). As contrasts, ZH alone and free
162 Cur were all carried out. To eliminate the effect of introduced ethanol, equivalent volume of ethanol
163 was added in each case. The freshly prepared samples were diluted 100 times with deionized water.
164 One drop of a diluted sample was placed on a freshly glow-discharged carbon film on a 400-mesh
165 copper grid and then stained with 1% uranyl acetate.

166 **Study of the interactions by spectroscopy**

167 The fluorescence spectra were recorded using an F7000 fluorescence spectrophotometer (Hitachi
168 Co., Japan). The fluorescence of Cur was measured by fixing its concentration at 2 µg/mL and
169 varying the concentrations of ZH from 0 to 5 mg/mL. The emission spectra were recorded from 450
170 to 650 nm with an excitation wavelength of 425 nm. Similarly, intrinsic fluorescence of ZH was
171 measured by fixing the concentration at 1 mg/mL and varying the concentrations of Cur from 0 to 30
172 µg/mL. Emission spectra were recorded from 290 to 450 nm at an excitation wavelength of 280 nm.
173 Quenching of protein fluorescence due to energy transferred from the tyrosine (Tyr) residue to Cur
174 served to determine the binding affinity. Fluorescence quenching is described according to the
175 Stern-Volmer equation (Eq.1) ²⁷: $F_0/F = 1 + k_q\tau_0[Q] = 1 + K_{SV}[Q]$. In this equation F_0 and F are the
176 fluorescence intensities in the absence and presence of Cur, respectively, $[Q]$ is the Cur concentration,

177 K_{SV} is the Stern-Volmer quenching constant, k_q is the bimolecular quenching rate constant, and τ_0 is
178 the lifetime of fluorescence in the absence of a quencher. Hence, Eq. 1 was applied to determine K_{SV}
179 by linear regression of a plot of F_0/F versus $[Q]$. Fluorescence quenching can be further classified as
180 dynamic or static quenching. In the case of static quenching, the quenching data can be analysed
181 according to a modified Stern-Volmer model (Eq. 2)²⁷: $F_0/\Delta F = F_0/(F_0-F) = 1/(faKa[-Q]) + 1/fa$. In
182 this equation fa is the fraction of accessible fluorescence, and Ka is the effective quenching constant
183 for the accessible fluorophores, and can be treated as an associative binding constant between a
184 quencher and an acceptor. The linear regression between $F_0/(F_0-F)$ and $1/[Q]$ enables the
185 determination of $1/faKa$ (slope) and $1/fa$ (intercept), and therefore Ka .

186 The freshly prepared nanocomplexes dispersion prepared in ZH solution (2.5 mg/mL) was
187 lyophilized under light-resistant condition by covering with foil paper before FTIR determination. As
188 contrasts, the powdered samples of Cur monomer and ZH were also prepared. FTIR spectra were
189 measured on a Nicolet Avatar 360 FTIR spectrometer with a 4 cm^{-1} resolution and 64 scans between
190 wavenumbers of 4000 cm^{-1} and 400 cm^{-1} . The powdered samples were prepared as KBr disks with 1
191 mg of the samples in 100 mg of KBr.

192 **Statistical Analysis**

193 Unless otherwise specified, all measurements were carried out in triplicate, and an analysis of
194 variance (ANOVA) of the data was performed using the SPSS 19.0 statistical analysis system. The
195 Duncan Test was used for comparison of mean values among the three treatments using a level of
196 significance of 5%.

197

198

199 **Results and discussion**

200 **Preparation and Characterization of ZH**

201 The enzymolysis efficiency plays a key role in preparation of ZH. As an alkaline endopeptidate,
202 *Alcalase* have high efficiency and low cost operation in proteins digestion. Thus, *Alcalase* has been
203 widely used in the enzymolysis of zein or corn protein meal.^{20, 28, 29} Water solubility of zein at
204 different incubation time is shown in Fig. 1A. With incubation time increasing, the water solubility
205 of zein gradually increased, and a plateau was achieved after 2 h hydrolysis. This liquefaction
206 process of zein as a function of incubation time can be clearly seen from Fig.1A (inset). After 1 h
207 incubation, zein was almost completely liquefied. Additionally, the hydrolysis treatment made
208 zeaxanthin released, which led to the hydrolysate solutions showed salmon pink and the color
209 became deeper with incubation time increasing.

210 This hydrolysis process was further monitored by DH (Fig.1B) and the electrophoretic patterns
211 (inset of Fig.1B). Native zein was composed of two polypeptides, which matched the MW of α -zein
212 (21 and 25 kDa).³⁰ The result indicates that commercial zein is composed primarily of α -zein. This
213 finding is well supported by previous report.³¹ The two polypeptides of α -zein are all susceptible to
214 *Alcalase* (Fig. 1B), showing a steady degradation over the incubation time. In the first 1 h, DH was
215 rapidly increased accompanying with incubation time and the electrophoretic patterns were quickly
216 receded. Over the next 2 h, the DH was increased from 14.4% to 19%, and native proteinic bands
217 completely disappeared. The HPLC-MS results further indicate that the molecular weight of ZH is
218 almost all below 1000 Da (see supporting information). These findings are in line with the previous
219 report, where *Alcalase*-treated ZH yielded three major fractions with estimated MMs of 640, 354 and
220 251 Da.³² Additionally, the enzymolysis of *Alcalase* don't appreciably change the percentage of most

221 amino acids in the soluble fractions of ZH.²⁰

222 **Amphiphilic characteristics of ZH**

223 Pyrene fluorescence probe was used for studying self-assembly properties of ZH. Pyrene is an
224 uncharged hydrophobic molecule, whose fluorescence is strongly influenced by the polarity of its
225 local environment. Pyrene has a very low solubility in water, and its concentration in saturated
226 aqueous solutions has been reported to be either 3.8×10^{-7} M or 7.0×10^{-7} M.^{33, 34} Pyrene could
227 selectively solubilize in hydrophobic regions or microphases existing in aqueous medium. The
228 vibration fine structure of its monomer fluorescence spectra in solution makes pyrene an excellent
229 probe to monitor the changes of local environment polarity.²⁴ The intensity ratio of the first peak to
230 the third (I1/I3) of fluorescence spectrum of pyrene shows the micro-environmental polarity where
231 the probe exists.³⁵ The abrupt change of I1/I3 as a function of surfactant concentrations has been
232 commonly used to determine CMC of the surfactant solution.²⁴ Fig. 2A shows the intensity ratios of
233 I1/I3 against ZH concentrations in PBs buffer. The value of I1/I3 was gradually decreased with
234 increasing ZH concentrations, and a plateau in the I1/I3 vs ZH concentrations plots appeared beyond
235 10 mg/mL. The CMC of ZH1 and ZH3 (hydrolysates acquired from 1 or 3 h hydrolysis) in aqueous
236 solution were found to be 1.14 and 1.63 mg/mL. This result means that ZH obtained at different
237 hydrolysis time all have the micelles formation capacity. Additionally, the CMC of ZH1 was slightly
238 less than that of ZH3, suggesting stronger micelles formation capacity for ZH1. This results may be
239 attribute to the stronger hydrophobic properties of ZH1, which can be confirmed by the peaks time of
240 RP-HPLC (see supporting information)

241 The micelles formation of ZH in water may be attributed to special amino acid sequence of
242 α -zein. α -Zein contains a large number of hydrophobic amino acids (>60%), and its subunits (Z19,

243 Z22) are well-known for highly repeated homologous sequence³⁶. *Alcalase* is an endoproteinase,
244 which has a high specificity for aromatic (Phe, Trp, and Tyr), acidic (Glu), sulfur-containing (Met),
245 and aliphatic (Leu and Ala).³⁷ This suggests that the proteolysis of zein by *Alcalase* could result in
246 plenty of amphipathic polypeptide fragments appearances, which likely lead to the formation of ZH
247 micelles in water solution.

248 Excellent interfacial properties (foaming and emulsification) for many peptides or protein
249 hydrolysates (e. g., corn gluten hydrolysates²⁸ and rice bran protein hydrolysates³⁸) have been
250 reported. Surfactin, which refers to a bacterial cyclic lipopeptide, can reduce the surface tension of
251 air-water from 72 mN m⁻¹ to 27 mN m⁻¹ at a low concentration.³⁹ The time evolution of surface
252 tension for ZH1, ZH3 and Na-Cas at the oil-water interface are shown in Fig.2B. The surface
253 tensions of ZH1, ZH3 and Na-Cas were gradually decreased with the increase of adsorption time in 2
254 h, which can be associated with surfactant substance adsorption at the interface. Na-Cas is an
255 excellent surfactant with good emulsifying property in practice, and this can be proved by the
256 reduction of surface tension at oil-water interface. ZH1 and ZH3 both showed prominent surface
257 tension reduction capacity, although they cannot compare with Na-Cas. It indicates that ZHs
258 prepared in different hydrolysis time have the same strong interfacial active.

259 **Water solubility and chemical stability of ZH-Cur nanocomplexes**

260 ZH displays great potential applications in solubilization of hydrophobic actives and in
261 nanoparticles delivery systems due to its amphiphilic characteristics. Hence, Cur was chose as a
262 model to study the complexation between ZH and Cur. The absorption spectra of free Cur, ZH alone
263 and ZH-Cur mixture in PBs are presented in Fig. 3A. Because of poor solubility, free Cur in PBs has
264 only a weak absorption peak at 425 nm. However, the absorbance intensity of ZH-Cur mixture is

265 considerably increased. Additionally, the results also showed that ZH has no absorbance at this
266 wavelength. These results indirectly indicate that Cur could be solubilized hugely due to the
267 existence of ZH. The appearances of Cur in pure PBs and ZH solutions can be observed in Fig. 3B
268 (inset). The free Cur in PBs was very turbid due to its poor water solubility. However, the existence
269 of ZH tremendously solubilized Cur, and the ZH-Cur mixture solutions displayed yellow and highly
270 transparent appearances. The water solubility of Cur could reach up to 90 $\mu\text{g}/\text{mL}$ (Fig. 3B) when the
271 ZH concentration is above 2.5 mg/mL , which is increased about 32 times compared with that of free
272 Cur in PBs (2.9 $\mu\text{g}/\text{mL}$). However, according to previously reported results (11 ng/mL),^{40, 41} Cur
273 solubility is increased 8200-fold by this anti-solvent process in ZH solutions. It needs to point out
274 that Cur solubility also has a great increase in PBs after this anti-solvent process. A similar result has
275 been previously reported, in which the Cur solubility in water is 3.14 $\mu\text{g}/\text{mL}$ after a similar
276 anti-solvent treatment.⁸ Additionally, it can be calculated that the encapsulation efficiency of Cur can
277 reach up to 90% when ZH concentration is above 2.5 mg/mL . Therefore, ZH could be utilized as a
278 solubilizer for Cur, and it may be suitable for development of Cur-enriched clear beverages. The
279 solubilization of Cur in ZH solutions could attribute to the entrapment of Cur in hydrophobic core of
280 ZH micelles, which hugely limited intermolecular aggregations of Cur.

281 Fig.3C shows the short-time storage stability of Cur in ZH solutions with different concentrations.
282 The result showed that free Cur in PBs was very unstable, and only 4% Cur was retained after 24 h
283 storage at ambient conditions. This result is well supported by previous report that the degradation of
284 free Cur is usually very fast under neutral-basic conditions.^{42, 43} As expected, the stability of Cur in
285 the presence of ZH was greatly improved. Cur was very stable in the initial 12 h, in spite of the
286 stability slowly decreased with further extension of storage time. Final retained ratio of Cur was still

287 above 60% in ZH solution with a concentration of 5 mg/mL. In fact, after 15 days storage at 4 °C
288 under light resistant conditions, the retained ratios of Cur in ZH solutions (2.5 and 5 mg/mL) were all
289 above 90% (data not shown). The possible mechanisms for stabilization of Cur in ZH solutions may
290 be explained as follows. Firstly, the “immobilization” of Cur by binding to ZH is decreased its
291 mobility and consequently its chemical reactivity. Another one is the physical barrier against
292 penetration of oxidizing agents and UV-light, whose accessibility to Cur is hindered by the
293 entrapment in ZH micelles. A similar report can be found in the literature, in which the author
294 suggest that the presence of a hydrophobic zein matrix around Cur provides protection against the
295 damaging effects of UV radiations by minimizing the interaction of light rays with the entrapped
296 molecules.⁴⁴ Besides, the prominent antioxidative effect of ZH may also play a role in protection of
297 Cur from degradation.

298 **Colloidal characteristics of ZH-Cur nanocomplexes**

299 The colloid stability of ZH-Cur nanocomplexes can be characterized by their particle size and
300 zeta potential. Generally, smaller size and higher zeta potential mean prominent colloid stability. The
301 volume-weighted particle size distribution and zeta potential of ZH alone and ZH-Cur
302 nanocomplexes are shown in Fig. 4. ZH had a wide size distribution from tens to hundreds of
303 nanometers in PBs and its zeta potential was approximate to -40 mV. The particle size of free Cur
304 was micron-sized in PBs and its zeta potential was about -25 mV, which indicate that the Cur
305 particles are unstable in long time storage. In fact, after hours standing at ambient conditions, Cur
306 aggregation and precipitation happened. However, Cur in ZH solutions resulted in the formation of
307 monodispersed nanoparticles (diameters <50 nm), and the zeta potential was increased from -25 to
308 -45 mV based on ZH concentrations (Fig. 4B). The results indicate that Cur particles in ZH solutions

309 become more uniform and stable. In fact, the particle size of ZH-Cur nanocomplexes in ZH solutions
310 with the concentrations of 2.5 and 5 mg/mL had no any change in 15 days (data not shown), after
311 stored at 4 °C and light resistant conditions. A similar result has been found for Na-Cas stabilized
312 Cur nanoparticles.⁴⁵ However, the size scale of ZH based Cur particles is far smaller comparing with
313 the Na-Cas based particles (150 nm). This may be attributed to the fact that the molecular weight of
314 ZH is much smaller than that of Na-Cas.

315 The morphologies of free Cur, ZH alone and ZH-Cur nanocomplexes in water solution were
316 observed by TEM (Fig. 5). Due to low water solubility, larger aggregates (Fig. 5A) of free Cur could
317 be easily observed. The sphere-like ZH aggregates (Fig. 5B) with size scales of 20 to 100 nm,
318 displayed a high degree of polydispersity, which could be regarded as the morphologies of ZH
319 micelles. The image of ZH-Cur nanocomplexes is shown in Fig. 5C. Interestingly, the
320 nanocomplexes were transparent in TEM image and showed regular spherical structures with small
321 diameters (<50 nm). This result is very in line with the previous DLS results (Fig. 4A). In addition, it
322 can be observed that a plenty of smaller black spots appeared around the transparent particles in the
323 image (Fig. 5C). This phenomenon may be attributed to the adsorption of small Cur aggregates on
324 the surface of ZH-Cur nanocomplexes.

325 **Complexation of ZH with Cur**

326 The intrinsic fluorescence of proteins has been widely used to investigate the binding of drug
327 molecules to proteins in solutions. Fluorescence of Tyr residues can be emitted at the excitation
328 wavelength of 280 nm. Our previous study indicates that ZH have a strong fluorescence emission
329 peak at around 305 nm upon excitation at 280 nm. The fluorescence emission spectra of ZH in the
330 presence of different Cur concentrations are shown in Fig. 6A. The intensity of the fluorescence

331 emission of ZH at around 305 nm was gradually decreased with the increase of Cur concentrations,
332 and the maximum emission wavelength remained unchanged. These results indicate that there are no
333 changes in the local dielectric environment of Tyr residues, and Cur molecules might bind to any or
334 all of Tyr residues through hydrophobic interactions. The previous report on fluorescence study of
335 Cur-casein micelles complexation well support these results.⁴⁶

336 The use of fluorescence in binding study requires attention to the possibility of non-binding
337 induced (dynamic) quenching.¹ To judge quenching models, the fluorescence quenching data were
338 analysed using the Stern-Volmer Eq.1. The values of K_{sv} and k_q for the system were calculated to be
339 $1.54 \times 10^8 \text{ M}^{-1}$ and $1.54 \times 10^{13} \text{ M}^{-1}\text{s}^{-1}$, respectively, which were much higher than maximal dynamic
340 quenching constant ($2.0 \times 10^{10} \text{ M}^{-1} \text{ s}^{-1}$). This indicates that the quenching process between ZH and
341 Cur is mainly due to static quenching by the formation of the ZH-Cur complexes. The effective
342 quenching constant K_a was calculated using the modified Stern-Volmer Eq. 2, and the corresponding
343 K_a value ($1.35 \times 10^4 \text{ M}^{-1}$) is given in Fig. 6A (inset), suggesting the strong interactions between ZH
344 and Cur in aqueous phase. Similar results about the interactions between proteins and Cur have been
345 reported previously.^{46, 47}

346 The fluorescence of Cur is very sensitive to the polarity of its surrounding environment. We used
347 intrinsic fluorescence spectroscopy of Cur to study the photophysical properties of Cur in the
348 presence of ZH (Fig. 6B). The results showed that only a low-intensity broad fluorescence peak at
349 around 550 nm appeared, when free Cur was excited at 425 nm in absence of ZH. Small increments
350 of ZH resulted in a sharper fluorescence peak with increased intensity and a blue-shift in maximum
351 emission wavelength of Cur (from ~550 nm to ~ 500 nm). This phenomenon could be further support
352 by previous report, in which the incorporation of pigment (Cur) in colloidal particles result in a blue

353 shift by 10 nm and a prominent hypochromic effect.⁴⁴ The blue-shift and increment of fluorescence
354 intensity indicate the movement of Cur from a polar to a less polar micro-environment. The results
355 are in good agreement with previous reports, where Cur is bound with various proteins, such as
356 α_{S1} -casein, casein micelles and human serum albumin.^{43, 46, 48} The authors all suggest that the
357 increment and blue-shift of fluorescence signal is attributed to the binding of Cur with the
358 hydrophobic regions of protein molecules. Additionally, some previous study also indicate that
359 proline-rich protein (PRP) could interact with polyphenol by hydrophobic interactions with the
360 pyrrolidine ring of proline.⁴⁹ Zein is a PRP too, and its hydrolysate contains 12% proline residuals.²⁰
361 Hence, there is thus a possibility that Cur could bind to the pyrrolidine ring of proline.

362 The FTIR spectra of Cur monomer, ZH alone and the complexes of ZH and Cur are shown in Fig.
363 6C. The characteristic absorbance peak around 3510cm^{-1} , corresponding to the -OH stretching
364 vibration of Cur, disappeared after the binding of ZH with Cur. Moreover, the number and intensity
365 of absorbance peaks in the fingerprint region of Cur obviously reduced after the complexation
366 between ZH and Cur. Compared with ZH alone, there was a shift of the absorbance peak from 1540
367 to 1542 cm^{-1} after binding with Cur, and the peak of ZH at 1658 cm^{-1} also shifted to 1655cm^{-1} . The
368 results suggest that Cur possibly bind together with the amide I group of ZH. A similar result has
369 been reported by *Kang Pan, et al.*⁴⁵

370 Conclusions

371 With amphiphilic characteristic, ZH tend to self-assemble into micelles in water solution, leading
372 to strong hydrophobic complexation of ZH with Cur molecules, as confirmed by the spectroscopy
373 analyses. The complexation remarkably increased the water solubility of Cur, moreover, the chemical
374 stability of Cur during storage under ambient conditions also considerably improved. The ZH-Cur

375 nanocomplexes are nano-scale (diameter <50 nm) in water solution, its dispersions are transparent
376 and displayed a good colloidal stability. Compared with native zein, ZH maybe turn into a better
377 vehicle to delivery water-insoluble bioactive compounds, because ZH itself has a beneficial effect on
378 bodies. Thus, ZH could be used as a new nano-delivery vehicle for Cur, which gives a solution for
379 preparation of Cur-enriched functional beverages.

380 **Acknowledgements**

381 This research was supported by grants from the Chinese National Natural Science Foundation
382 (Serial numbers: 31130042), the Project of National Key Technology Research and Development
383 Program for the National High Technology Research and Development Program of China (863
384 Program: 2013AA102208), and Special Fund for Grain-Scientific Research in the Public Interest
385 (201313005, 201303071), Science and Technology Achievements Transformation Projects of
386 Guangdong Higher Education Institutes (2013CXZDC003).

387

388

389 **Referances**

- 390 1. G. Israeli-Lev and Y. D. Livney, *Food Hydrocolloids*, 2014, 35, 28-35.
- 391 2. P. Anand, A. B. Kunnumakkara, R. A. Newman and B. B. Aggarwal, *Mol. Pharm.*, 2007, 4, 807-818.
- 392 3. R. R. Balandrán-Quintana, M. A. Valdéz-Covarrubias, A. M. Mendoza-Wilson and R. R. Sotelo-Mundo,
393 *International Dairy Journal*, 2013, 32, 133-135.
- 394 4. Y. Luo and Q. Wang, *Journal of Applied Polymer Science*, 2014, 131, 40696.
- 395 5. A. R. Patel and K. P. Velikov, *Current Opinion in Colloid & Interface Science*, 2014, 19, 450-458.
- 396 6. K.-K. Li, X. Zhang, Q. Huang, S.-W. Yin, X.-Q. Yang, Q.-B. Wen, C.-H. Tang and F.-R. Lai, *Journal of Food*
397 *Engineering*, 2014, 127, 103-110.
- 398 7. K.-K. Li, S.-W. Yin, Y.-C. Yin, C.-H. Tang, X.-Q. Yang and S.-H. Wen, *Journal of Food Engineering*, 2013, 119,
399 343-352.
- 400 8. A. Patel, Y. Hu, J. K. Tiwari and K. P. Velikov, *Soft Matter*, 2010, 6, 6192-6199.
- 401 9. A. R. Patel, P. Heussen, J. Hazekamp, E. Drost and K. P. Velikov, *Food Chemistry*, 2012, 133, 423-429.
- 402 10. T. Zou, Z. Li, S. S. Percival, S. Bonard and L. Gu, *Food hydrocolloids*, 2012, 27, 293-300.
- 403 11. N. Parris, P. H. Cooke and K. B. Hicks, *J. Agric. Food Chem.*, 2005, 53, 4788-4792.
- 404 12. A. R. Patel, E. C. Bouwens and K. P. Velikov, *J. Agric. Food Chem.*, 2010, 58, 12497-12503.
- 405 13. H. Chen and Q. Zhong, *Food Hydrocolloids*, 2015, 43, 593-602.

- 406 14. K. Rajagopal and J. P. Schneider, *Curr. Opin. Struct. Biol.*, 2004, 14, 480-486.
- 407 15. J. Fernández - Carneado, M. J. Kogan, S. Castel and E. Giralte, *Angewandte Chemie International Edition*, 2004,
408 43, 1811-1814.
- 409 16. P. Esmaeilzadeh, G. Hause, F. Heyroth, B. Fuhrmann, B. Ahrens, T. Groth and Z. Fakhroueian, *Journal of*
410 *Chemical Engineering and Chemistry Research*, 2014, 1, 24-32.
- 411 17. S. Singh, *Cell*, 2007, 130, 765-768.
- 412 18. A. Goel, A. B. Kunnumakkara and B. B. Aggarwal, *Biochem. Pharmacol.*, 2008, 75, 787-809.
- 413 19. K. Letchford, R. Liggins and H. Burt, *J. Pharm. Sci.*, 2008, 97, 1179-1190.
- 414 20. B. Kong and Y. L. Xiong, *J. Agric. Food Chem.*, 2006, 54, 6059-6068.
- 415 21. A. G. Gornall, C. J. Bardawill and M. M. David, *Determination of serum proteins by means of the biuret reaction*,
416 1949.
- 417 22. J. Adler-Nissen, *Enzymic hydrolysis of food proteins*, Elsevier Applied Science Publishers, 1986.
- 418 23. U. K. Laemmli, *Nature*, 1970, 227, 680-685.
- 419 24. Y. Liu and R. Guo, *Biophys. Chem.*, 2008, 136, 67-73.
- 420 25. F. Tamm, G. Sauer, M. Scampicchio and S. Drusch, *Food Hydrocolloids*, 2012, 27, 371-377.
- 421 26. R. A. Holland, J. L. Kirschvink, T. G. Doak and M. Wikelski, *PLoS One*, 2008, 3, e1676, 1671-1676.
- 422 27. J. R. Lakowicz and B. R. Masters, *Journal of Biomedical Optics*, 2008, 13, 9901.
- 423 28. A. Mannheim and M. Cheryan, *J. Am. Oil Chem. Soc.*, 1992, 69, 1163-1169.
- 424 29. J. E. Hardwick and C. E. Glatz, *J. Agric. Food Chem.*, 1989, 37, 1188-1192.
- 425 30. A. Esen, *Journal of cereal science*, 1987.
- 426 31. T. J. Anderson and B. P. Lamsal, *Cereal Chemistry*, 2011, 88, 159-173.
- 427 32. X. Tang, Z. He, Y. Dai, Y. L. Xiong, M. Xie and J. Chen, *J. Agric. Food Chem.*, 2009, 58, 587-593.
- 428 33. M. Štěpánek, K. Krijtova, K. Prochazka, Y. Teng, S. Webber and P. Munk, *Acta polymerica*, 1998, 49, 96-102.
- 429 34. A. Yekta, B. Xu, J. Duhamel, H. Adiwidjaja and M. A. Winnik, *Macromolecules*, 1995, 28, 956-966.
- 430 35. C. Keyes-Baig, J. Duhamel, S.-Y. Fung, J. Bezaire and P. Chen, *J. Am. Chem. Soc.*, 2004, 126, 7522-7532.
- 431 36. P. Argos, K. Pedersen, M. Marks and B. Larkins, *J. Biol. Chem.*, 1982, 257, 9984-9990.
- 432 37. D. Doucet, D. E. Otter, S. F. Gauthier and E. A. Foegeding, *J. Agric. Food Chem.*, 2003, 51, 6300-6308.
- 433 38. J. Hamada, *J. Food Sci.*, 2000, 65, 305-310.
- 434 39. F. Peypoux, J. Bonmatin and J. Wallach, *Appl. Microbiol. Biotechnol.*, 1999, 51, 553-563.
- 435 40. Y. Kaminaga, A. Nagatsu, T. Akiyama, N. Sugimoto, T. Yamazaki, T. Maitani and H. Mizukami, *FEBS Lett.*, 2003,
436 555, 311-316.
- 437 41. H. Sasaki, Y. Sunagawa, K. Takahashi, A. Imaizumi, H. Fukuda, T. Hashimoto, H. Wada, Y. Katanasaka, H. Kakeya
438 and M. Fujita, *Biol. Pharm. Bull.*, 2011, 34, 660-665.
- 439 42. Y.-J. Wang, M.-H. Pan, A.-L. Cheng, L.-I. Lin, Y.-S. Ho, C.-Y. Hsieh and J.-K. Lin, *J. Pharm. Biomed. Anal.*, 1997, 15,
440 1867-1876.
- 441 43. A. H. Sneharani, S. A. Singh and A. Appu Rao, *J. Agric. Food Chem.*, 2009, 57, 10386-10391.
- 442 44. A. Patel, P. Heussen, E. Dorst, J. Hazekamp and K. P. Velikov, *Food chemistry*, 2013, 141, 1466-1471.
- 443 45. K. Pan, Q. Zhong and S. J. Baek, *J. Agric. Food Chem.*, 2013, 61, 6036-6043.
- 444 46. A. Sahu, N. Kasoju and U. Bora, *Biomacromolecules*, 2008, 9, 2905-2912.
- 445 47. P. Bourassa, C. Kanakis, P. Tarantilis, M. Pollissiou and H. Tajmir-Riahi, *The Journal of Physical Chemistry B*, 2010,
446 114, 3348-3354.
- 447 48. M. H. Leung and T. W. Kee, *Langmuir*, 2009, 25, 5773-5777.
- 448 49. N. J. Baxter, T. H. Lilley, E. Haslam and M. P. Williamson, *Biochemistry*, 1997, 36, 5566-5577.

449

Figure captions

Fig. 1 A: Water solubility of zein at different incubation time. Different letters (a-e) above the bars indicate significant difference ($p < 0.05$) in mean. The inset shows the appearances of zein suspensions at specified incubation time. B: Hydrolysis degree as a function of incubation time. The inset shows the SDS-PAGE of zein in different incubation time (lane 1 is native α -zein, and lane 2-6 are ZH after 10, 30, 60, 120, and 180 min incubation). The arrows in the inset indicate the subunits of α -zein (21 and 25 kDa).

Fig. 2 A: Pyrene fluorescence ratio of I1:I3 as a function of ZH1 and ZH3 concentrations. ZH1 and ZH3 represent ZHs obtained after 1 and 3 h hydrolysis. B: Surface tensions of ZH1, ZH3 and Na-Cas at oil-water interface against adsorption time. The concentration of each sample is 1 mg/mL.

Fig. 3 A: UV-vis absorbance spectra of ZH alone (red), free Cur (black), and ZH-Cur mixture (blue). B: Solubility of Cur in ZH solutions with different concentrations. Different letters (a-c) above the bars indicate significant difference ($p < 0.05$) in mean. Inset: Appearances of Cur dispersions in ZH solutions with different concentrations. C: Residual ratios of Cur as a function of storage time at ambient conditions.

Fig. 4 Typical size distribution (A) and zeta potential (B) of ZH alone and ZH-Cur nanocomplexes in ZH solutions with different concentrations. Different letters (a-d) above the bars indicate significant difference ($p < 0.05$) in mean.

Fig. 5 Typical TEM images of free Cur (A), ZH alone (B) and ZH-Cur complexes (C) with 3.0 k \times , 15.0 k \times , and 25.0 k \times magnification respectively.

Fig. 6 A: Intrinsic fluorescence of ZH in the presence of different concentrations of Cur. Inset: Modified Stern-Volmer plots describing fluorescence quenching of ZH in the presence of Cur. B: Fluorescence spectra of Cur with varying concentrations of ZH. C: FTIR spectra of free Cur (blue), ZH alone (red), and ZH-Cur complexes (ZH-Cur, black). Arrows (in Fig. A and B) indicate the concentration increasing trend of ZH or Cur.

Fig. 1

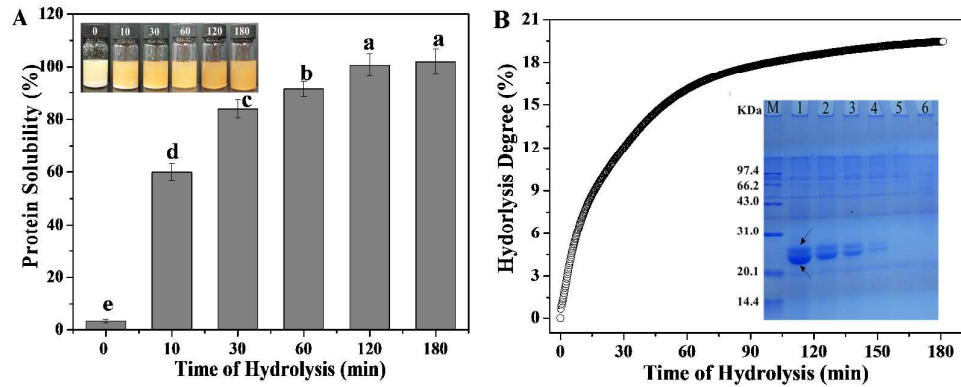


Fig. 2

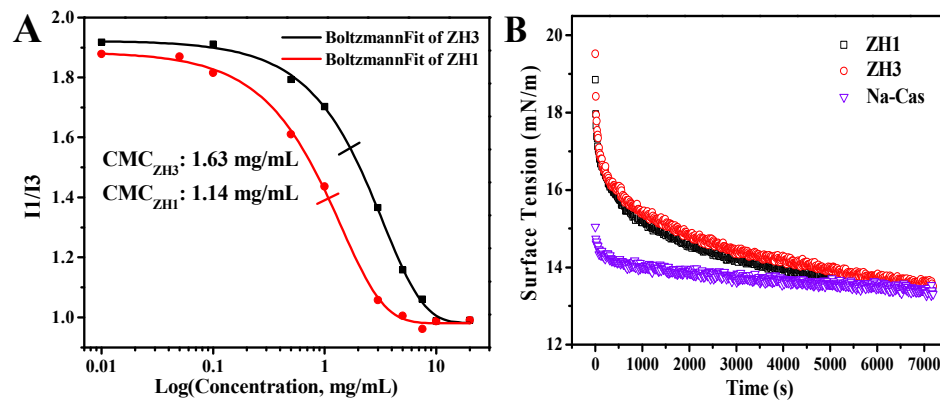


Fig. 3

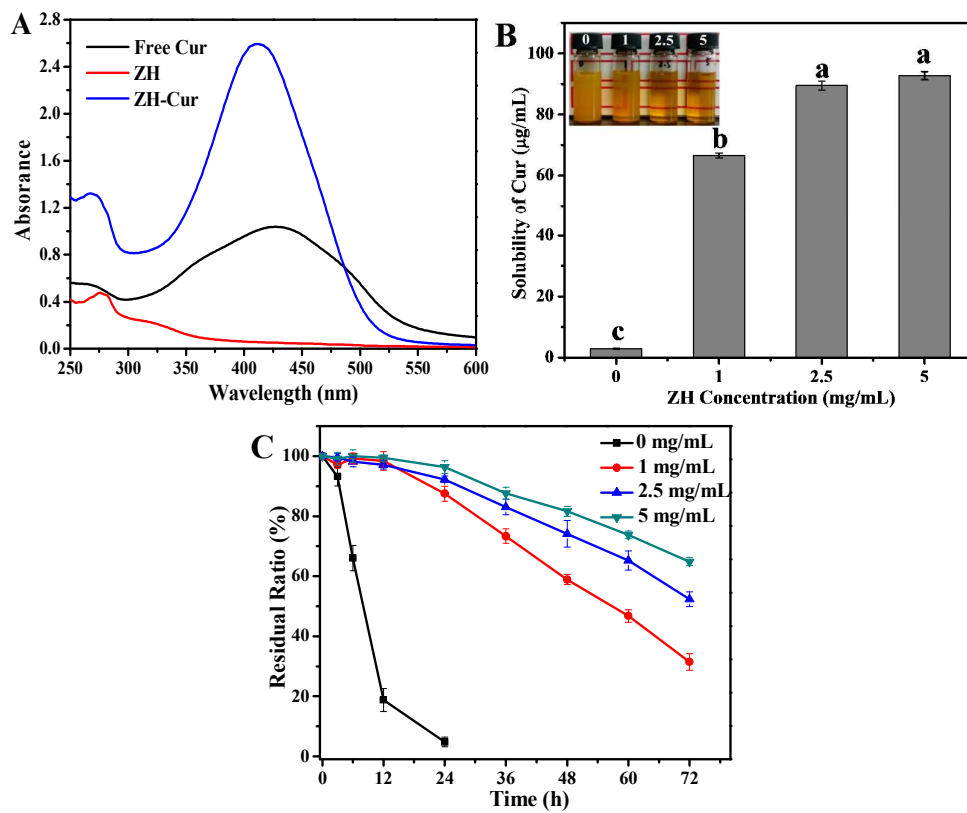


Fig. 4

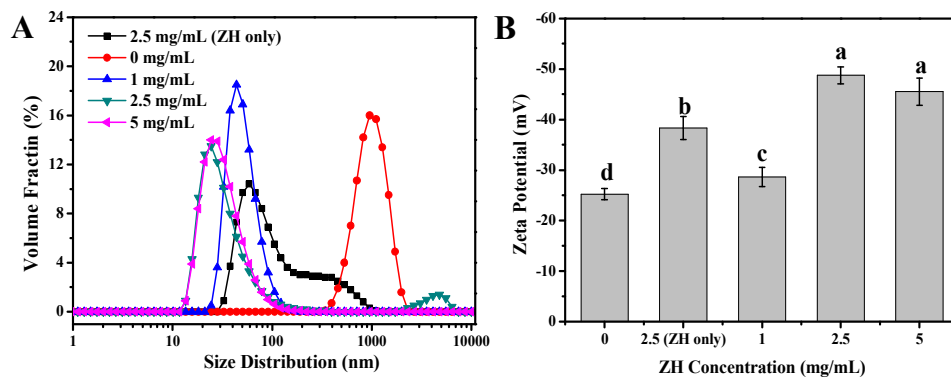


Fig. 5

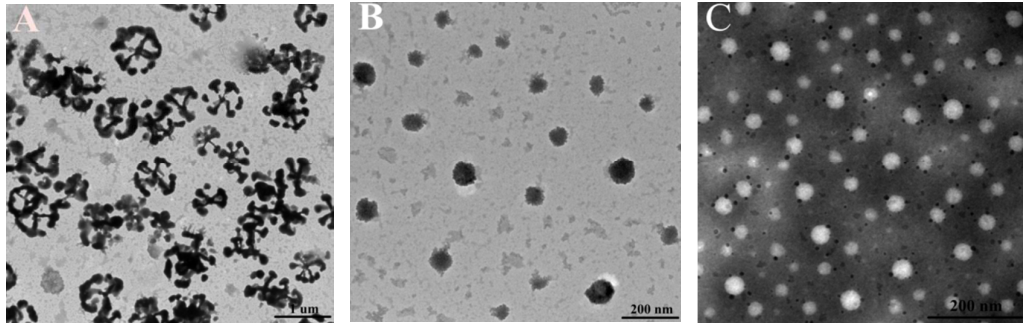
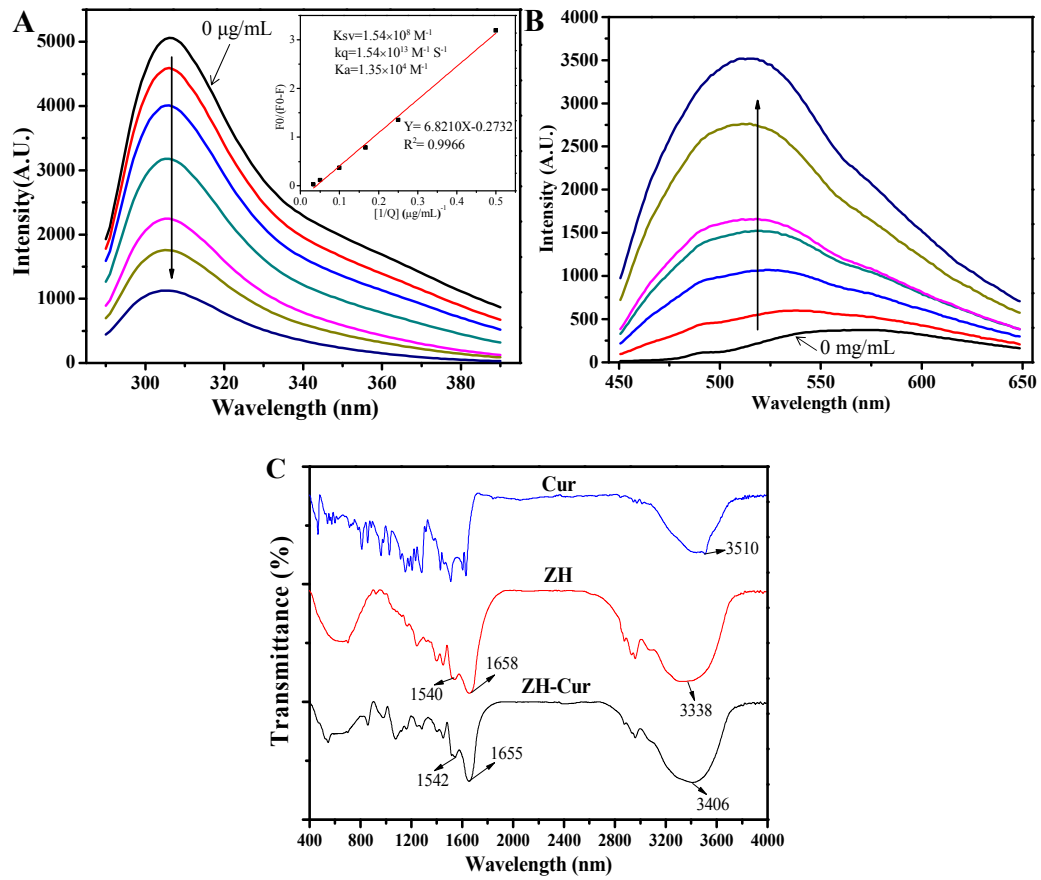


Fig. 6



Graphical Abstract

In this paper, we developed amphiphilic zein hydrolysate (ZH) as a novel delivery vehicle, which could be used for preparation of curcumin (Cur)-loaded nanoparticles by a simple anti-solvent method. These particles have a small size (<50 nm) and its dispersion in aqueous solution is transparent, which could have a great application potential in nutraceutical-fortified food and clear beverages. Spectroscopic studies showed that the formation of these nanoparticles mainly attribute to strong hydrophobic complexation between ZH and Cur.

